Glucose Regulated Protein 78 Diminishes α-Synuclein Neurotoxicity in a Rat Model of Parkinson Disease

Marina S Gorbatyuk[1,2], Arseniy Shabashvili[1], Weijun Chen[1,3], Craig Meyers[1,3], Layla F Sullivan[1], Max Salganik[1,3], Jonathan H Lin[4], Alfred S Lewin[1,5], Nicholas Muzyczka[1,3,5,6] and Oleg S Gorbatyuk[1,3,5,6]

[1]Department of Molecular Genetics and Microbiology, College of Medicine, University of Florida, Gainesville, Florida, USA; [2]Department of Cell Biology and Anatomy, University of North Texas, Health Science Center North Texas Eye Research Institute, Fort Worth, Texas, USA; [3]UF Genetics Institute, College of Medicine, University of Florida, Gainesville, Florida, USA; [4]Department of Pathology, University of California, La Jolla, California, USA; [5]The Powell Gene Therapy Center, College of Medicine, University of Florida, Gainesville, Florida, USA; [6]McKnight Brain Institute, College of Medicine, University of Florida, Gainesville, Florida, USA

Accumulation of human wild-type (wt) α-synuclein (α-syn) induces neurodegeneration in humans and in experimental rodent models of Parkinson disease (PD). It also leads to endoplasmic reticulum (ER) stress and activation of the unfolded protein response (UPR). We overexpressed glucose regulated protein 78, also known as BiP (GRP78/BiP), to test the hypothesis that this ER chaperone modulates the UPR, blocks apoptosis, and promotes the survival of nigral dopamine (DA) neurons in a rat model of PD induced by elevated level of human α-syn. We determined that α-syn activates ER stress mediators associated with pancreatic ER kinase-like ER kinase (PERK) and activating transcription factor-6 (ATF6) signaling pathways as well as proaoptotic CCAAT/-enhancer-binding protein homologous protein (CHOP) in nigral DA neurons. At the same time, overexpression of GRP78/BiP diminished α-syn neurotoxicity by down regulating ER stress mediators and the level of apoptosis, promoted survival of nigral tyrosine hydroxylase (TH) positive cells and resulted in higher levels of striatal DA, while eliminating amphetamine induced behavioral asymmetry. We also detected a complex between GRP78/BiP and α-syn that may contribute to prevention of the neurotoxicity caused by α-syn. Our data suggest that the molecular chaperone GRP78/BiP plays a neuroprotective role in α-syn-induced Parkinson-like neurodegeneration.

INTRODUCTION

Idiopathic Parkinson disease (PD) is a progressive neurodegenerative disorder characterized by a loss of dopamine (DA)-producing neurons in the substantia nigra pars compacta (SNc), and accompanied by depletion of DA level in the striatum.[1,2] Age is the major risk factor for the development and progression of PD. Aging affects many cellular processes that predispose to Parkinson-like neurodegeneration. One such process is the sustained increase of α-synuclein (α-syn) protein level during aging, which in the absence of an efficient proteasome system, results in protein misfolding and accumulation.[3] A robust age-related, nigra-specific increase in α-syn protein and a specific loss of tyrosine hydroxylase (TH) positive neurons were shown in monkeys and humans.[4,5] Recombinant adeno-associated virus (rAAV)-mediated overexpression of human wild-type (wt) α-syn in rat SNc has been found to induce progressive nigrostriatal degeneration with α-syn-positive cytoplasmic and axonal inclusions, and dystrophic and fragmented neuritis leading to cell death in rat model of PD.[6] In transgenic mice it has also been demonstrated that overexpression of wt α-syn may lead to neuropathological changes and axonal degeneration.[5,7] In spite of intensive study, it is not clear how α-syn causes neurodegeneration. Apparently, abundant α-syn protein is less efficiently cleared from neuronal cytosol, leading to its accumulation and Lewy body formation. Accumulation of unfolded and/or misfolded proteins in the endoplasmic reticulum (ER) lumen induces ER stress, which is defined as an imbalance between the cellular demand for ER function and ER capacity.[8–10] The ER stress response, also termed the unfolded protein response (UPR), serves to protect cells against the toxic build-up of un-/misfolded proteins.[11,12] The first step in the UPR is the recognition of unfolded proteins by the HSP70-class chaperone glucose regulated protein 78, also known as BiP (GRP78/BiP). The titration of GRP78/BiP by unfolded proteins leads to its dissociation from, and activation of the three ER stress receptors: pancreatic ER kinase-like ER kinase (PERK), activating transcription factor-6 (ATF6), and inositol-requiring enzyme 1 (IRE1).[13] As reviewed by Szegezdi *et al.*, the PERK pathway is activated first, followed rapidly by ATF6, while IRE1 is activated last. Phosphorylation of eukaryotic initiation factor 2α (eIF2α), the next mediator of the PERK pathway, leads to the blocking of general cap- or eIF2α-dependent protein synthesis (adaptive stage) in an attempt to restore cellular homeostasis. Internal ribosomal entry site-dependant translation allows ATF4 to escape eIF2α translational regulation and translocate to the nucleus. The ATF6 pathway, a second arm of the UPR,

Correspondence: Oleg S Gorbatyuk, Department of Molecular Genetics and Microbiology, College of Medicine, UF Genetics Institute, Gene Therapy Center, Cancer/Genetics Research Complex, Building, 2033 Mowry Rd, Rm CG-215, Gainesville, FL 32610. E-mail: olegor@ufl.edu

is initiated upon dissociation of ATF6 from GRP78, followed by its trafficking to the Golgi and subsequent proteolytic processing. This activation regulates the expression of ER chaperones and X box-binding protein 1 (XBP1), another transcription factor. To achieve its active form, XBP1 must undergo mRNA splicing, which is carried out by IRE1. Spliced XBP1 protein (sXBP1) translocates to the nucleus and controls the transcription of chaperones, co-chaperones and the PERK-inhibitor P58[IPK]. This concerted action aims to restore ER function by blocking further build-up of client proteins, enhancing the folding capacity and initiating degradation of protein aggregates. However, if homeostasis is not re-established after these steps, IRE1α signaling and then ATF6α signaling are attenuated, creating an imbalance in which proapoptotic output guides the cell toward apoptosis. The transcription factor C/EBP homologous protein (CHOP), the downstream regulator of the UPR, whose induction strongly depends on ATF4, promotes apoptotic cell death. It is an important element of the switch from prosurvival to prodeath signaling.[14] Therefore, its expression strongly correlates with a decision of the cell to commit suicide. Proapoptotic factors at this point would be attenuated by the relatively longer mRNA and protein half-lives of factors such as GRP78/BiP.[15,16]

Studies on postmortem brain samples have shown that immunoreactivity for the UPR activation markers, phosphorylated PERK and eIF2α (peIF2α), is detected in neuromelanin containing DA neurons in the SNc of PD patients but not in control cases.[17] In addition, phosphorylated PERK immunoreactivity is colocalized with increased α-syn in DA neurons.[17] Recent evidence showed that GRP78/BiP and peIF2α levels were elevated in cells overexpressing A53T-mutated α-syn,[18] suggesting that a change in α-syn, known to induce the familial form of PD, may result in the activation of the UPR pathway. Although two studies showed that the overexpression of human wt α-syn can induce the activation of UPR in yeast[19] and that α-syn toxicity is dependent on the phosphorylation at Ser129 which induces the UPR,[20] it remains to be clarified whether α-syn accumulation within the ER can directly induce the UPR and the consequent proapoptotic changes.[21] Despite the recent data demonstrating that the UPR is closely associated with α-syn increase and aggregation[21,22] and that pharmacological manipulation of ER stress attenuates protein misfolding in animal models of PD,[23] little remains known about activation of individual UPR pathways and individual ER stress markers associated with PD pathology. In our recent study of autosomal dominant retinitis pigmentosa caused by the misfolded protein rhodopsin, we have demonstrated an involvement of ER stress signaling in degeneration of neuronal photoreceptor cells that could be ameliorated by overexpression of GRP78/BiP protein. Overexpression of GRP78/BiP reprograms ER stress signaling and blocks apoptosis.[24] This finding raised the possibility that overexpression of GRP78/BiP in nigral neurons might have a similar protective effect.

With respect to α-syn-induced pathology, there is direct evidence that GRP78/BiP forms a complex with α-syn and that GRP78/BiP levels are increased in cell as well as animal models showing aggregated α-syn accumulation.[21] Moreover, α-syn accumulation induces ATF4 expression indicating that the activation of UPR pathways in the PD brain is associated with α-syn

accumulation occurring in part within the ER.[21] In addition, it has been demonstrated that aging leads to a significant decline in GRP78/BiP expression (up to 40%) and activity in both brain and hepatic tissues of old versus young rodents, and this decline is thought to contribute to age-related impairments in cellular function.[25–30]

In this study we investigated the involvement of ER stress signaling in degeneration of nigral DA cells caused by α-syn-induced pathology. We demonstrated that the overexpression of GRP78/BiP protein diminishes α-syn cytotoxicity by reprogramming ER stress signaling pathways and eliminating apoptosis in the experimental model of Parkinson-like degeneration.

RESULTS

To study the role of α-syn overexpression in promoting ER stress, we injected rAAV expressing human α-syn into rat SNc. We used the rAAV serotype 5 capsid that allowed for α-syn overexpression in the SNc and the striatum of rats at 2–10 times above normal levels, depending on vector dosage and promoter strength. In the case of α-syn, injections were done in the right SNc, while the left was kept as a nontransduced internal control (**Figure 1a**). Judging by the pattern of staining, human wt α-syn expression level was approximately uniform over the SNc. Quantitative immunoblots of nigral tissues showed (**Figure 1b**) that human α-syn was expressed at 3.8 (±0.3%; $n = 4$) fold over the endogenous rat α-syn at 4 weeks after injection, when normalized to total protein. The antibody
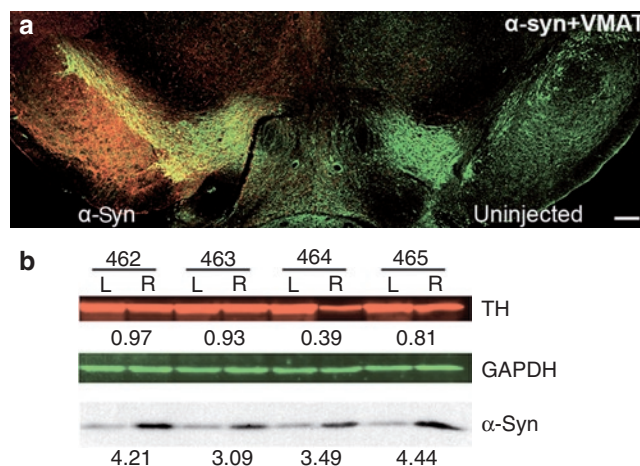

Figure 1 **The expression of the human wild-type (wt) α-synuclein (α-syn) in the substantia nigra pars compacta (SNc) in 4 weeks after recombinant adeno-associated virus (rAAV) injection.** (**a**) Photomicrographs showing the expression of the human wt α-syn transgene on the injected side of rat brain. α-Syn (red) was expressed in the majority of the tyrosine hydroxylase (TH)-positive neurons (green) in SNc and also can be seen in cells of the mesenphalic tegmentum and in the SN pars reticulate. Bar = 0.5 mm. (**b**) Measurement of α-syn and TH expression in animals that had been injected with human wt α-syn at 4 weeks postinjection. Samples of nigral extracts taken from the uninjected left side (L) and injected right side (R) of individual animals (462-465) were electrophoresed on acrylamide gels. Fifty micrograms of tissue extract was analyzed by immunoblots using antibodies that recognize both human and rat α-syn, as well as TH or GAPDH antibodies. The amount of TH enzyme was normalized to GAPDH and the ratio of the injected versus uninjected sides was calculated. The ratio of α-syn on the injected and uninjected sides was calculated for each animal using the same approach.

that was used bound to human and rat α-syn with the same affinity allowing direct comparison (**Supplementary Figure S1**). The 3.8-fold increase in α-syn expression is comparable to the increase seen in α-syn mRNA in PD patients.[4,31]

Overexpression of human wt α-syn in rat SNc activated the UPR

We used dissected SNc tissues from rats sacrificed at 4 weeks after injection of rAAV α-syn or rAAV green fluorescent protein (GFP) in the right SNc. Tissues from the left side were used as internal controls, and data obtained in experimental animals are expressed as percentage of injected side versus uninjected side. We chose the 4 weeks time point based on our previous studies demonstrating that this point correlates with maximum expression level of rAAV mediated vectors but does not yet result in significant neurodegeneration.[32–34] As expected, unbiased estimation of TH-positive cells in the SNc at 4 weeks did not reveal significant neuronal loss in animals that had been injected with α-syn as compared to GFP-injected rats (79.4 ± 11.9%, $n = 7$ versus 95.4 ± 8.2%, $n = 6$; $P > 0.05$). We also found that in hemispheres injected with rAAV α-syn the level of nigral TH protein was not reduced significantly (**Figure 1b**). Thus, we confirmed our previous results[33,34] that human wt α-syn does not induce significant neuronal death at this early time point and, therefore, we expected to be able to detect an elevation of the ER stress markers corresponding to a persistent ER stress response in the SNc. We determined that overexpression of human wt α-syn activated the ER stress signaling by upregulation of mediators of at least two pathways: ATF6 and PERK (**Figure 2**, see also **Supplementary Figure S2**). We found that the expression level of phosphorylated eIF2α (peIF2α) in α-syn-injected animals was elevated compared to GFP-injected rats (123 ± 3.7%, $n = 4$ versus 99.8 ± 4.75%, $n = 4$; $P < 0.05$). Another hallmark of the PERK pathway, the ATF4 protein, was upregulated in α-syn-injected SNc by ninefold compared to GFP-injected rats (704 ± 14.3%, $n = 5$ versus 74 ± 28%, $n = 4$; $P < 0.001$). The ATF6 pathway was also affected. Cleaved phosphorylated ATF6 (pATF6) protein was significantly increased in α-syn-injected SNc compared to GFP injected animals (242 ± 12.4%, $n = 6$ versus 92 ± 5.5%, $n = 4$; $P < 0.05$). Control injections with AAV GFP did not cause the activation of any of these markers, indicating that viral infection or the effects of surgery were not responsible for the elevated UPR response.

Given that both the PERK and ATF6 pathways were upregulated it was not surprising to find that the expression level of proapoptotic CHOP protein (**Figure 2**) was dramatically increased in brains injected with α-syn compared to GFP-injected animals (395 ± 63.5%, $n = 6$ versus 128 ± 20.2%, $n = 4$; $P < 0.01$). sXbp1, the hallmark of the IRE1 pathway, also showed a trend to increase in α-syn expressing rats compared to sXBP1 protein in GFP injected rats (115.0 ± 10.8% versus 99.7 ± 4.8%, both $n = 4$); however, the increase did not reach significance.

Gene delivery of GRP78/BiP reduces apoptosis caused by overexpression of human wt α-syn

There is growing evidence that the mechanism of α-syn neurotoxicity promotes cell death through apoptosis.[35] We showed previously that increased expression of GRP78/BiP protein downregulates the proapoptotic CHOP/GADD153 protein and reduces
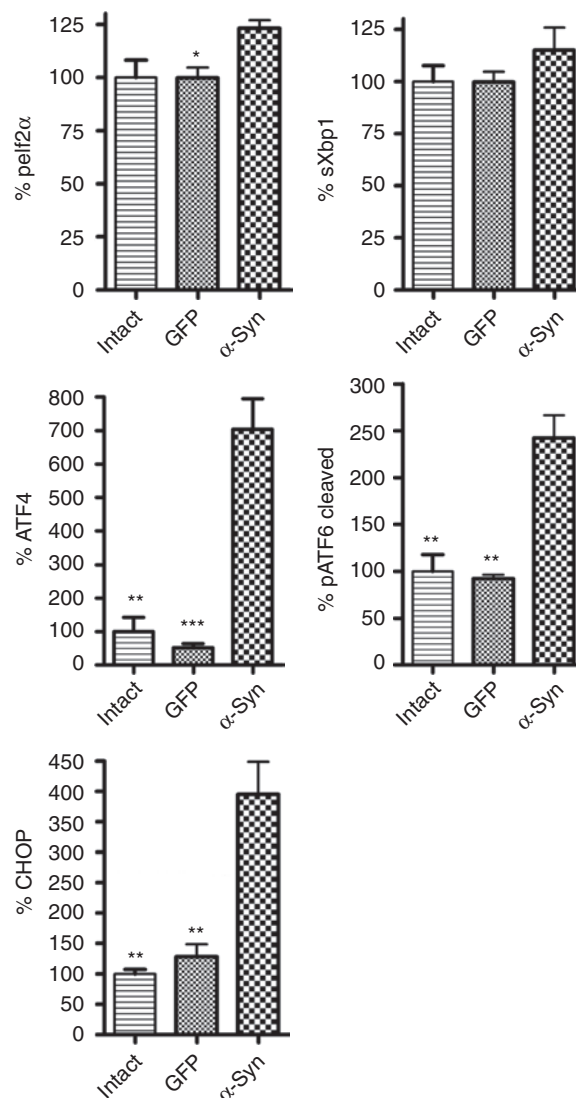

Figure 2 Immunoblot analysis of the unfolded protein response (UPR) markers in nigral tissue at 4 weeks after recombinant adeno-associated virus (rAAV) human wild-type (wt) α-synuclein (α-syn) and rAAV green fluorescent protein (GFP) injections. Overexpression of human α-syn in the substantia nigra pars compacta (SNc) at 4 weeks postinjection leads to a significant upregulation of peIF2α, ATF4, and pATF6 (50 kDa) proteins. The activation of these UPR mediators results a significant overexpression of the proapoptotic C/EBP homologous protein (CHOP) protein. Tukey's *post hoc* results are indicated as *, **, ***$P < 0.05$, 0.01, and 0.001, respectively versus α-syn; $n = 4$–6 for each group.

levels of apoptosis caused by misfolded rhodopsin.[24] It was, therefore, logical to examine the ability of GRP78/BiP protein to reduce apoptosis in DA cells expressing α-syn. To quantify the protective effect of GRP78/BiP protein on apoptosis we used a nucleosome release assay that measures mono- and oligonucleosomes in the cytoplasmic fraction of cell lysates, a hallmark of cell death via apoptosis. SH-SY5Y cells transfected with plasmids expressing human wt α-syn alone or in a combination with GRP78/BiP were compared with mock transfected cells. In α-syn-expressing cells, there was an elevation in nucleosome release by 50% (±8.98%, both $n = 4$; $P < 0.05$). However, cotransfection of cells with both

α-syn and GRP78/BiP protein-expressing plasmids eliminated this increase and reduced the signal down to that observed in mock transfected cells (**Figure 3a**). Overexpression of GRP78/BiP protein in SH-SY5Y cells alone did not lead to nucleosome release. We concluded that expression of human wt α-syn promotes apoptosis and an elevated level of GRP78/BiP eliminates this effect.

To determine whether the antiapoptotic effect of GRP78/BiP involved interaction with α-syn, we coexpressed human wt α-syn and a Flag-tagged BiP protein (Flag-tag was placed in front of a KDEL fragment as in our previous work[24]) in SH-SY5Y cells. Precipitation of human α-syn from a total protein extract of SH-SY5Y cells with mouse antibody against human α-syn also precipitated GRP78/BiP protein, which was detected with anti-Flag antibody (**Figure 3b**).

Simultaneous viral delivery of human wt α-syn and GRP78/BiP into SNc leads to increased expression of both proteins

Since increased expression of GRP78/BiP can suppress α-syn-mediated apoptosis and appears to bind to α-syn, at least *in vitro*, we launched a study to validate its therapeutic potential

in the α-syn rat model of PD. For this purpose, we coinjected both rAAV BiP and rAAV α-syn simultaneously or injected a single virus expressing only GRP78/BiP, human wt α-syn or GFP. To provide evidence that there is no a competition between two viral vectors delivered simultaneously, we carried out preliminary experiments in which three groups of rats were injected with rAAV α-syn, rAAV BiP-Flag or both.

Immunostained images of sections from animals expressing BiP-Flag alone or both BiP-Flag and α-syn are shown in **Figure 4a** and **b**, respectively. Antibody specific to Flag and human α-syn were used to confirm expression of both exogenous proteins in nigral DA neurons identified by vesicle monoamine transporter-2 immunostaining. Western blot analysis of nigral tissue samples revealed that combined injection of α-syn and BiP-Flag virus did not significantly change the level of expression of either protein compared to injection of either expression vector alone (**Figure 4c**). The expression level of α-syn in SNc injected with AAV α-syn + BiP was 0.87 of the level seen when α-syn alone was injected, and the level of BiP-Flag in mixed injections was 1.07 of that seen when BiP-Flag was injected alone. As expected, immunoblotting of pooled ($n = 4$) nigral protein extract revealed an increase of total GRP78/BiP expression up to 39% on the injected side compared to the uninjected side (**Figure 4d**).

To confirm that GRP78/BiP is a binding partner of human wt α-syn *in vivo*, we pooled protein extracts obtained from individual SNcs injected with both BiP-Flag and α-syn virus. Immunoprecipitation of pooled protein extracts from injected brains with anti-Flag antibody also precipitated α-syn, demonstrating that GRP78/BiP binds to human wt α-syn *in vivo* as well as *in vitro* (**Figure 4e**).

Confocal microscopy revealed mostly diffused distribution of human wt α-syn over the cytoplasm of nigral DA neurons in rats injected with both rAAV α-syn alone (**Figure 5a–d**) or rAAV α-syn + rAAV BiP-Flag (**Figure 5i–h**). However, α-syn in neurons injected with rAAV α-syn alone was more prone to accumulation. Immunocytochemistry with antibodies specific to Flag visualized localization of BiP-Flag protein to the ER of DA neurons as seen by calnexin staining (**Figure 5e–h**). However, Flag is not exclusively colocalized with calnexin as seen in **Figure 5g**. Since the level of localization of both proteins is not the focus of this study the quantitation was not performed. Also due to the diffuse distribution of overexpressed human wt α-syn throughout the cytoplasm, including the ER (calnexin), confocal microscopy was of limited use in defining precise localization of α-syn to the ER.

Overexpression of GRP78/BiP protein led to reprogramming of the ER stress response in the rat SNc

In previous work, we showed that ectopic α-syn expression in SNc resulted in a slight loss of TH neurons at 4 weeks (see above) and a statistically significant loss (~50%) at 8 weeks postinjection.[33,34] To determine whether increased expression of GRP78/BiP protein could alleviate this pathology, rAAV BiP virus that did not contain the Flag sequence was injected at the same time as rAAV α-syn. At 4 weeks, western blot analysis of striatal tissues confirmed that exogenous GRP78/BiP did not affect expression of exogenous human α-syn, when both rAAV α-syn and rAAV BiP were injected together, compared to single injection of rAAV
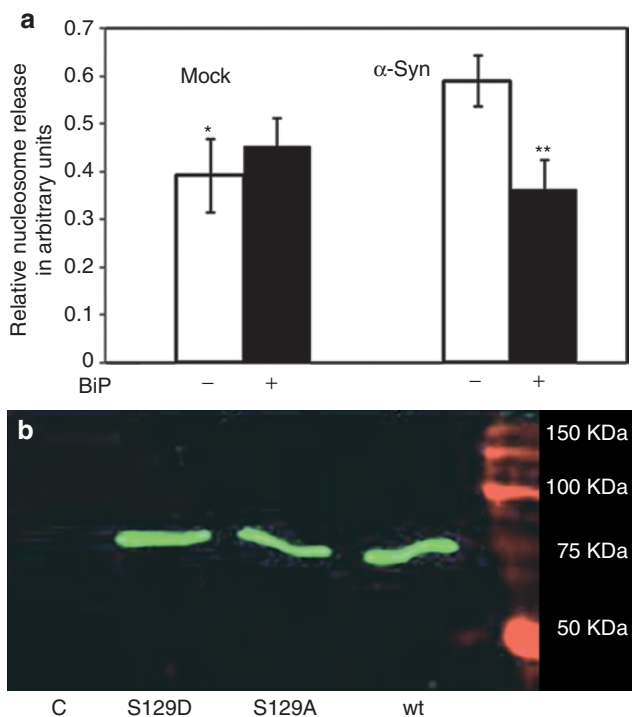

Figure 3 Human wild-type (wt) α-synuclein (α-syn) and GRP78/BiP cotransfection of SH-SY5Y cells. (**a**) GRP78/BiP overexpression protects SH-SY5Y cells from apoptosis induced by human wt α-syn. Apoptotic signal was measured in 48 hours by nucleosome release ELISA assay. Unpaired *t*-test is indicated as **$P < 0.01$; $n = 4$. (**b**) Overexpressed BiP binds to the human wt α-syn. Detection of BiP-Flag (green band) by anti-Flag Ab in a protein extract from SH-SY5Y coexpressing BiP-Flag and human wt α-syn was performed by immunoprecipitation with the human α-syn-specific antibody. Western blot analysis detected the band corresponding to 78 kDa by Odyssey Infrared System. The two additional mutants shown (S129A and S129D), while not related to this study, demonstrate that GRP78 can interact with both the phosphorylated (S129D) and nonphosphorylated forms of wt α-syn. As a negative control (C) for the precipitation study mouse anti-green fluorescent protein (GFP) antibody was used instead of human wt α-syn antibody.
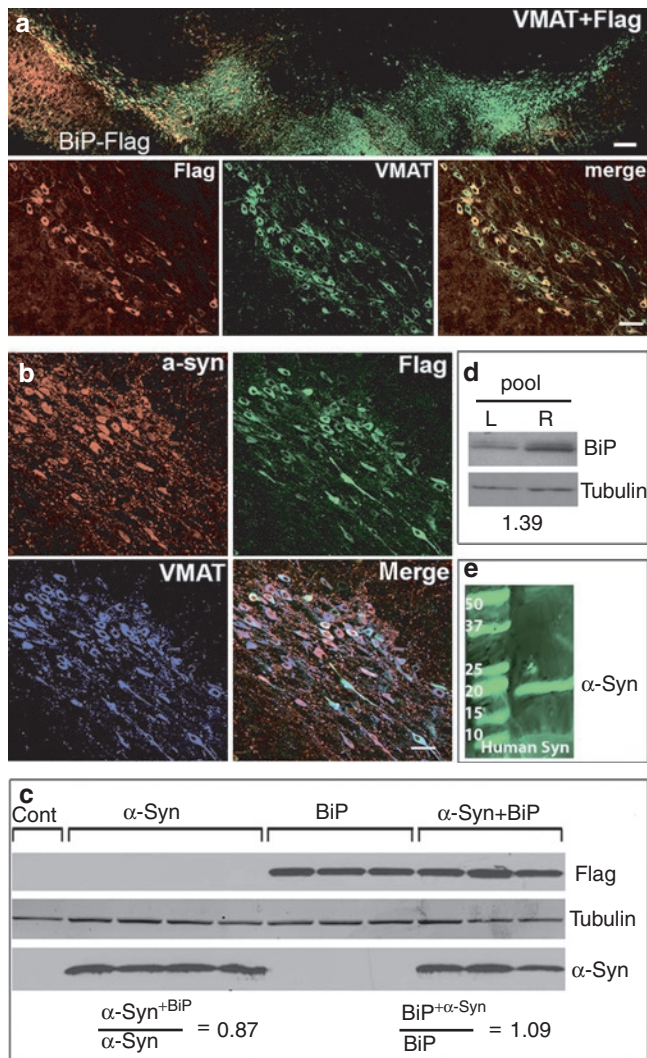
Figure 4 **Expression of BiP-Flag and human α-synuclein (α-syn) in rat substantia nigra pars compacta (SNc).** (**a**) Images of the SNc expressing BiP-Flag protein alone on a side of injection. Left side (top image) was intact and did not demonstrate staining with Flag-specific antibodies (bar = 150 μm). In red—detection of Flag-tag with Cy3-conjugated secondary Ab, in green—detection of the vesicle monoamine transporter-2 (VMAT) with Cy2-conjugated secondary Ab. Higher resolution images (bottom) show BiP-Flag expression in most if not all nigral dopamine (DA) neurons (bar = 25 μm). (**b**) Coexpression of both BiP-Flag and human wild-type (wt) α-syn was found in SNc of rats injected with both viruses (bar = 25 μm). (**c**) Coexpression of BiP-Flag and human α-syn do not inhibit an expression level of each other. Expression level of BiP-Flag or human α-syn in a dual injection is equivalent to one with a single viral injection. Western blot (WB) visualized with an antibody specific to Flag and human α-syn. "Cont" is noninjected side of single rat taken as a control. (**d**) Nigral tissue from 4 weeks animals was extracted and pooled (n = 4) and then immunoblotted with antibody to the GRP78/BiP. A loading control (tubulin) is also shown. Extracts from the uninjected side (L) were compared with the injected side (R). Expression of total GRP78/BiP protein detected with anti-GRP78/BiP antibody was about 39% higher in injected sides compared to uninjected. (**e**) Image of immunoblot of immunoprecipitated protein extract isolated from the SNc injected with a viral combination. Immunoprecipitation was done using anti-Flag antibody. The membrane from the immunoblot was treated with a specific antibody against human α-syn to detect the band corresponding to 19 kDa α-syn. As a negative control for the precipitation study mouse immunoglobulin was used instead of anti-Flag antibody (data not shown).
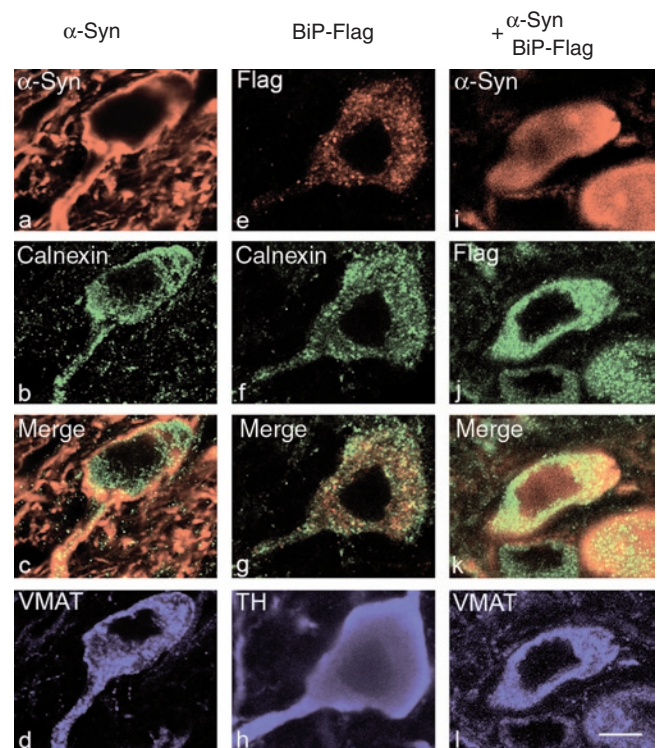

Figure 5 **Confocal microscopy of representative cells in substantia nigra pars compacta (SNc) of rats at 4 weeks after injections of (a–d) recombinant adeno-associated virus (rAAV) α-synuclein (α-syn) alone, (e–h) rAAV BiP-Flag alone, or (i–l) both α-syn and BiP-Flag vectors.** (**a–d**) SNc neuron expressing α-syn alone detected with antibody specific to human wild-type (wt) α-syn (red). The image shows localization of accumulating α-syn mostly along axonal and cell body membrane, and to lesser extend in cytosol (**a**). Immunocytochemical detection of endoplasmic reticulum (ER) marker, calnexin (green) (**b**) revealed that α-syn might accumulate partially on the ER (**c**). Vesicle monoamine transporter-2 (VMAT) immunostaining (blue) of the same cell confirms that colocalization was identified in nigral dopamine (DA) neuron (**d**). (**e–h**) Overexpression of BiP-Flag alone in SNc neuron detected with anti-Flag antibody (red). Immunostaining of the same cell for calnexin (green) (**f**) allowed for colocalization with the Flag antibody, as seen on merged image (**g**), primarily on ER (yellow). However, some dust like red staining can be also found outside of the ER suggesting that overexpressed BiP might escape ER recruitment. Immunostaining for tyrosine hydroxylase (TH) (blue) in the same cell was used as a marker of DA producing neuron in the SNc (**h**). (**i–l**) Nigral neuron expressing both human wt α-syn (red) (**i**) and BiP-Flag (green) (**j**). Note that α-syn immunoreactivity spreads diffusely (**i**) compared to overexpression of human α-syn alone (**a**). Bar = 5 μm.

α-syn (**Supplementary Figure S3**). We also dissected the SNc at this time point to analyze the main ER stress markers in protein extracts obtained from combined (rAAV α-syn and rAAV BiP) or individual injections with each gene (**Figure 6**). As expected, there was an increase of GRP78/BiP protein expression in nigral tissue of rats injected with rAAV BiP alone (146.9 ± 17.2, n = 3; P < 0.05) or rAAV BiP in combination with rAAV α-syn (150.1 ± 13.4, n = 4; P < 0.05) (**Supplementary Figure S4**). We found that AAV-mediated overexpression of GRP78/BiP reduced the levels of both cleaved pATF6 and ATF4 proteins (**Figure 6**). Expression of ATF4 protein dropped 41% when GFP78/BiP virus was coinjected with α-syn virus (704±14% versus 415±19%, both n = 5; P < 0.05). The cleaved pATF6 product (pATF6 50) was reduced

by 42% compared to injection with α-syn alone (242 ± 12%, $n = 6$ versus 141 ± 27%, $n = 5$; $P < 0.05$). This supported the hypothesis that overexpression of GRP78/BiP protein could reprogram the ER stress response *in vivo*.

Could however, reducing the expression levels of the two main ER stress hallmarks affect the expression level of proapoptotic CHOP protein? To determine this we analyzed protein extracts at 4 and 8 weeks from animals injected with α-syn alone or with a mixture of α-syn and GFP78/BiP (**Figure 6**). At 4 weeks, expression of CHOP protein was reduced 42% (395 ± 53%, $n = 6$ to 231 ± 33%, $n = 5$; $P < 0.05$) when rAAV BiP was combined with rAAV α-syn. At 8 weeks, the expression of CHOP protein was significantly downregulated by GRP78/BiP as well (152 ± 12% versus 84 ± 9%, both $n = 4$; $P < 0.001$). Thus, although the level of CHOP protein induced by α-syn was different at the two time points, in both cases the level of CHOP was significantly reduced by coexpression of BiP, and at 8 weeks, CHOP levels were essentially normal.
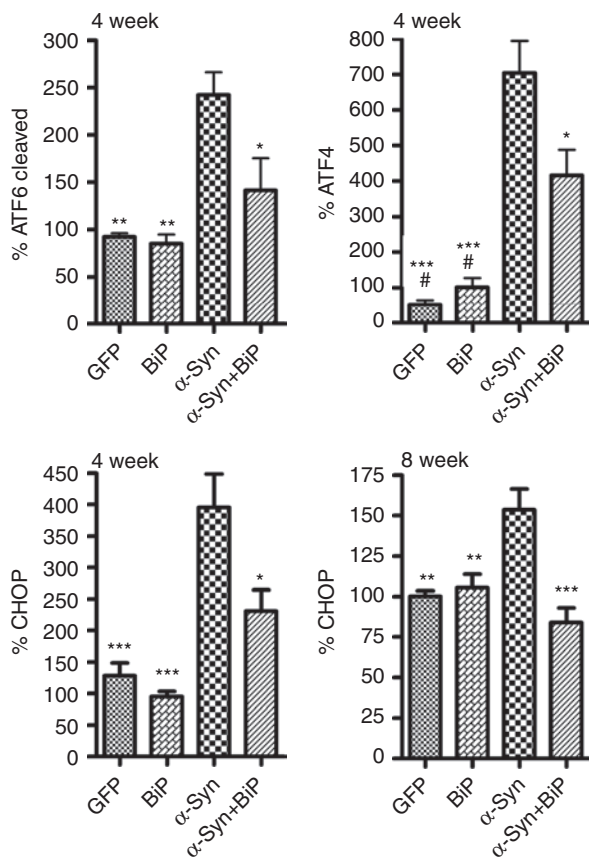

Figure 6 Overexpression of GRP78/BiP protein in the substantia nigra pars compacta (SNc) of Parkinson disease (PD) rats leads to reprogramming the endoplasmic reticulum (ER) stress signaling. At 4 weeks of PD progression GRP78/BiP significantly reduced accumulation of the ER stress hallmarks such as cleaved pATF6 (pATF6 50) and ATF4 (PERK pathway). Production of C/EBP homologous protein (CHOP) protein was also down regulated at 4 and 8 weeks in rat SNc injected with both α-synuclein (α-syn) and GRP78/BiP compared to SNc of rats injected with α-syn. Injection with recombinant adeno-associated virus (rAAV) BiP was not a statistically different from green fluorescent protein (GFP) injection or intact control. Tukey's *post hoc* results are indicated as *, **, ***$P < 0.05$, 0.01, and 0.001, respectively versus α-syn; #$P < 0.05$ versus α-syn + GRP78/BiP; $n = 4$–7 for each group.

Overexpression of GRP78/BiP prevented the loss of TH-positive neuronal cells and maintained DA level in the α-syn PD model

Previously, we found that there was a significant loss of striatal DA levels and TH-positive neurons in the SNc when α-syn was expressed in rat brains at 8 and 26 weeks postinjection.[6,32–34] To investigate whether expression of GRP78/BiP would reduce the level of neurodegeneration, we compared the striatal DA level and the number of TH-positive cells in SNc after single and combined viral injections at 4, 8, and 16 weeks postinjection (**Figure 7a–d**). We found that the number of TH-positive cells (**Figure 7a,b**) was reduced dramatically (52%) at 8 weeks in animals injected with α-syn alone compared to GFP control (100.6 ± 6.7%, $n = 4$ versus 48 ± 8.1%, $n = 11$; $P < 0.01$). However, overexpression of GRP78/BiP along with α-syn prevented much of the loss of TH-positive cells caused by α-syn overexpression (48 ± 8.1%, $n = 11$ versus 76.4 ± 6.1%, $n = 10$; $P < 0.05$). These animals exhibited only a 24% loss of TH-positive cells compared to GFP, which did not reach significance ($P > 0.05$). Moreover, the reduction in α-syn-induced loss of TH-positive neurons was maintained by GRP78/BiP at 16 weeks (34.36 ± 13.19%, $n = 5$ versus 74.51 ± 4.04%, $n = 6$; $P < 0.05$). GRP78/BiP overexpression alone did not cause a significant change in the number of TH-positive cells.

In parallel with counting of TH-positive cells, we also measured the level of DA in the striatum of injected animals (**Figure 7c,d**). Striatal DA declined at 8 weeks in rats injected with a single virus-expressing human α-syn compared to GFP-injected animals (25.9 ± 11.4%, $n = 6$ versus 98.5 ± 4.1%, $n = 10$; $P < 0.001$) and compared to a single GRP78/BiP injection (25.9 ± 11.4% versus 89.4 ± 4.6%, $n = 5$; $P < 0.001$). Here again, overexpression of GRP78/BiP along with α-syn significantly attenuated the loss of striatal DA compared with animals injected with α-syn alone (71.5 ± 8.1%, $n = 7$ versus, 25.9 ± 11.4%; $P < 0.01$). As in a case of TH-positive cells, overexpression of GRP78/BiP alone did not affect DA levels in the striatum compared to control GFP injections (98.5 ± 4.1% versus 89.4 ± 4.5%, $P > 0.05$) and positive effect of striatal DA levels by GRP78/BiP was maintained at 16 weeks (21.87 ± 3.26%, $n = 6$ versus 60.69 ± 11.25%, $n = 5$; $P < 0.01$) (**Figure 7d**).

Overexpression of GRP78/BiP eliminated behavior deficit in the rat model of α-syn-induced PD

At 4 weeks postinjection with AAV expressing GFP, GRP78/BiP, α-syn, or α-syn plus GRP78/BiP we did not see a significant difference in number of amphetamine induced rotations between the experimental groups. However, at 8 weeks following injection we found that only α-syn-injected animals demonstrated a significant number of rotations towards (positive numbers) the injected side compared to α-syn+GRP78/BiP or GRP78/BiP-injected animals (accordingly, 240 ± 72.9, $n = 8$ versus −74,6 ± 52.7, $n = 9$ or −24.4 ± 36.3, $n = 18$; both $P < 0.001$) (**Figure 7e,f**). At 16 weeks α-syn-injected animals continued to demonstrate a significant number of ipsilateral rotations compared to GFP, α-syn+GRP78/BiP and GRP78/BiP-injected animals (209.1 ± 56.6, $n = 11$ versus −28.0 ± 4.7, $n = 8$, versus −48.1 ± 80.9, $n = 8$; both $P < 0.05$ and versus 5.7 ± 25.4, $n = 16$, $P < 0.01$) (**Figure 7f**). Such ipsilateral rotations were consistent with a functional loss of TH neurons and striatal DA
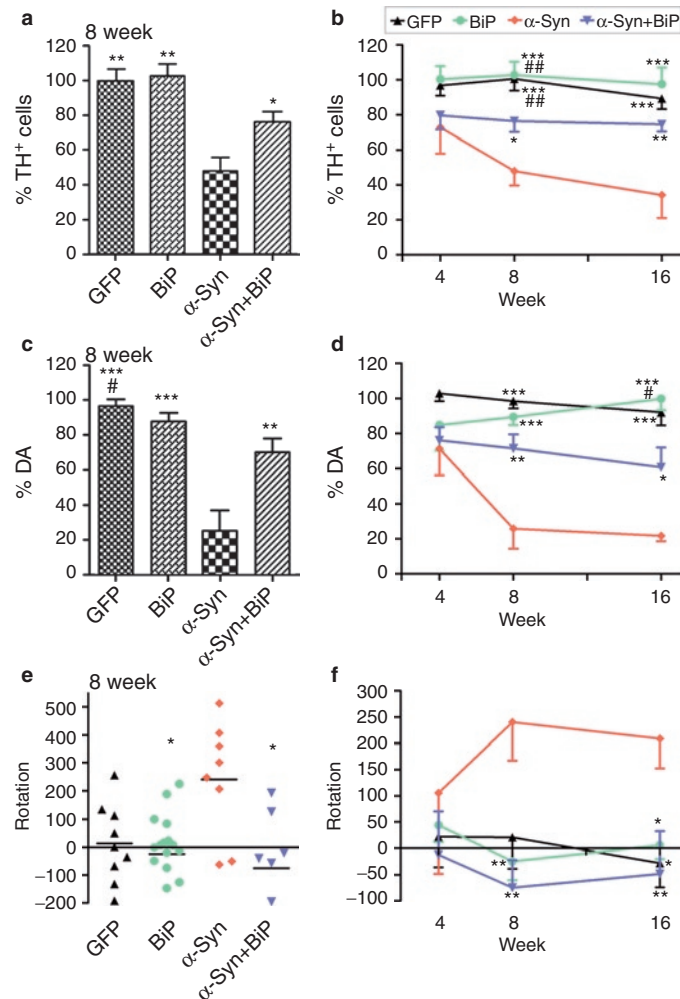
Figure 7 Overexpression of GRP78/BiP protein prevents loss of tyrosine hydroxylase (TH)-positive cells and striatal dopamine (DA) level as well as eliminates behavior deficit. (a) Unbiased estimation of TH$^+$ cells remaining in substantia nigra pars compacta (SNc) on the injected side as a percentage of the uninjected side ± SE at 8 weeks postinjection. A number of TH-positive neurons counted in α-synuclein (α-syn) injected SNc was dramatically reduced compared to control. However, coexpression of α-syn and GRP78/BiP proteins led to significant rescue of TH-positive cells preventing cell death compared to a single α-syn injection. These animals have only a 24% loss of TH-positive cells compared to green fluorescent protein (GFP) which was not statistically significant. GRP78/BiP overexpression alone did not reduce the number of TH-positive cells. One-way ANOVA analysis. Tukey *post hoc* results are indicated as *,**$P < 0.05$ and 0.01, respectively versus α-syn; $n = 4$–11 per group. **(b)** The graph shows the % TH+ cells remaining at different times postinjection. Two-way ANOVA statistics. Bonferroni post-tests are indicated as *, **, ***$P < 0.05$, 0.01, and 0.001, respectively versus α-syn; $^{##}P < 0.01$ versus α-syn + GRP78/BiP; $n = 4$–11 for each group at each time point. **(c)** At 8 weeks, decline of DA in the striatum injected with a virus expressing α-syn was 75% compared to GFP-injected animals. Overexpression of GRP78/BiP protein along with α-syn significantly (by 46%) preserved the dopamine (DA) level of injected animals observed in a single α-syn injection. This also was a statistically reliable from GFP control. Overexpression of GRP78/BiP protein alone did not block the synthesis of DA in injected SNcs compared to control GFP injection. One-way ANOVA analysis. Tukey *post hoc* results are indicated as **, ***$P < 0.01$, and 0.001, respectively versus α-syn; $^{#}P < 0.05$ versus α-syn + GRP78/BiP; $n = 5$–10 per group. **(d)** Changes in DA levels of different experimental group at 16 weeks were similar to 8 weeks. Two-way ANOVA statistics. Bonferroni post-tests are indicated as *,**,***$P < 0.05$, 0.01 and 0.001, respectively versus α-syn; $^{##}P < 0.01$ versus α-syn + GRP78/BiP; $n = 4$–10 for each group at each time point. **(e)** Amphetamine induced rotation test at 8 weeks revealed a significant number of rotations toward the injected side (positive, ipsilateral rotation) only in α-syn-injected rats compared to GRP78/BiP and α-syn plus GRP78/BiP. Amphetamine induced rotation was measured for 90 minutes and the average rotation plus SE is shown. One-way ANOVA analysis. Tukey's *post hoc* results are indicated as *$P < 0.05$ versus α-syn; $n = 9$–13 per group. **(f)** Amphetamine rotation versus time postinjection in α-syn-injected rats compared to GFP, GRP78/BiP, and α-syn plus GRP78/BiP. Two-way ANOVA analysis. Bonferroni post-test is indicated as *,**$P < 0.05$ and 0.01 versus α-syn; $n = 6$–18 per group.

in animals injected with α-syn alone, and a reduction in pathology when animals were coinjected with a GRP78/BiP-expressing virus.

DISCUSSION

The main purpose of this study was to investigate whether the mechanism of α-syn neurotoxicity in nigral DA neurons is

associated with an activation of the ER stress response, and to test the therapeutic potential of the antiapoptotic UPR chaperone GRP78/BiP for α-syn-induced PD progression. We used the rat model of PD in which human wt α-syn is overexpressed locally in the SNc. This model produces an average level of α-syn overexpression of 3.8-fold on the injected side of the brain (**Figure 1b**), which is similar to the increase in α-syn found in postmortem

PD brain tissue,[31] and produces measurable neurodegeneration at 8 weeks postinjection.

This increase in α-syn correlated with an increase in markers of two of the three pathways of the UPR at 4 weeks when α-syn expression reached maximum and significant neurodegeneration had not yet occurred. There was a 23% elevation of the peIf2α proteins and a ninefold induction of ATF4 (PERK pathway), and a greater than twofold elevation for cleaved pATF6 protein (ATF6 pathway) (**Figure 2** and **Supplementary Figure S2**). In addition, the proapoptotic CHOP protein, a downstream marker of ATF6 and PERK pathways, was dramatically increased (threefold) in injected SNc tissue. Elevation of this protein directly promotes apoptosis[36] resulting in DA neuronal cell death.[37] These results correlate with findings that were discovered in postmortem tissues from PD patients, which demonstrated that the PERK-related pathway of the UPR is activated in DA neurons bearing α-syn inclusions.[17] Taken together these facts suggest that the UPR is involved in DA neuron degeneration. Furthermore, this study has directly implicated wt α-syn accumulation in the activation of the UPR *in vivo* resulting in proapoptotic changes. Most importantly, overexpression of GRP78/BiP or GFP did not affect UPR activation markers analyzed in this study. Given that the titer of the rAAV GFP virus was approximately five times higher than that of—the human α-syn virus used in this study and that rAAV mediated overexpression of rat wt α-syn was shown to not induce nigral degeneration,[38] this suggests that α-syn-induced UPR activation was due specifically to the properties of human α-syn and not simply to a general overload of ER lumen capacity.

Previous studies in cultured cells that showed an increase in GRP78/BiP and peIF2α when a mutant of α-syn (A53T) was expressed are also consistent with our results.[18] Of note, sXBP1, a marker of the protective arm of the UPR was not significantly elevated at 4 weeks (**Figure 2**). In addition, we did not find a statistically significant difference in accumulation of GRP78/BiP protein in rAAV α-syn-injected SNc that often accompanies UPR initiation. There may be several reasons for this, but the most likely is that at 4 weeks we did not "catch" elevation of GRP78/BiP, because it had already returned to a normal level. We note also that activation of the UPR was induced by wt α-syn rather than a mutant, which leaves open the possibility that a mechanism other than α-syn misfolding may be associated with activation. Overexpression of α-syn leads to accumulation of free-fatty acids and reactive species[39,40] that are known to stimulate and perturb ER homeostasis resulting in general aberrant protein folding.[41] Therefore, future experiments might address a correlation between overexpression of α-syn and an oxidizing environment of the ER (protein disulfide isomerase, Ero1p), an accumulation of reactive oxygen species, and free-fatty acids in nigral TH neurons.

Currently, a growing body of evidence suggests that GRP78/BiP protein has a therapeutic potential by reduction of apoptosis in cultured cells.[42–44] In our previous study of autosomal dominant retinitis pigmentosa transgenic rats, we demonstrated that the GRP78/BiP protein promotes photoreceptor cell survival *in vivo* and protects cell from apoptosis.[24] It was logical, therefore, to test the hypothesis that GRP78/BiP protein will promote TH neuron survival during degeneration caused by α-syn toxicity.

We found that AAV delivery of GRP78/BiP cDNA led to only a 39% increase of GRP78/BiP protein level on the injected side. As mentioned elsewhere, one possible reason for this moderate elevation is the potential down regulation of endogenous BiP transcription in response to the exogenous gene delivered by AAV.[45] As previously shown, the level of GRP78/BiP protein was not elevated >20–40% when it was induced by BiP inducer X.[46] This characteristic of BiP is unlike that of calreticulin, and other ER proteins, which have been shown to be overexpressed 50–100-fold without any apparent negative feedback. Another potentially major explanation for the relatively moderate overexpression of GRP78/BiP in nigral tissue samples may be the presence of macro- and microglial cells, which cannot be infected by AAV5,[32] and thus dilute the average level of BiP detected in the region since they only express at basal levels. Despite this minor setback, we have found that the levels of GRP78/BiP expression attained in our study were sufficient to ameliorate α-syn neurotoxicity.

We found that expression of GRP78/BiP protein significantly reduced the α-syn-induced loss of TH-positive neurons in the SNc, the loss of striatal DA, and the amphetamine induced rotational deficit at 8 and 16 weeks postinjection. This was due at least in part to a direct interaction of GRP78/BiP and α-syn. Furthermore, overexpression of GRP78/BiP protein alone in naïve animals did not lead to a reduction of TH-positive cells, or a reduction in the level of DA, or a behavioral deficit. This suggests that overexpression of GRP78/BiP, at least in the rat SNc, is not associated with overt pathology. The fact that GRP78/BiP expression can attenuate α-syn-induced neurodegeneration, and is not itself associated with toxicity, suggests that GRP78/BiP is a potential therapeutic target for treatment of PD.

In addition, several other proteins were implicated in α-syn-induced neurodegeneration. The proapoptotic CHOP protein, a downstream marker of the ATF6 and PERK pathways, was dramatically increased (threefold) in injected SNc tissue. Elevation of this protein directly promotes apoptosis[36] resulting in DA neuronal cell death.[37] Recent studies have demonstrated that in the chronic MPP+ model of PD, CHOP is robustly expressed; however, the CHOP knockout mouse was not protected from the loss of neurons[47] following MPP+ treatment. In our AAV PD model with a gradual loss of TH neurons, the dampening of CHOP protein, a mediator of apoptosis, seems to be beneficial. Dramatic reduction of CHOP protein in response to modulation of the ATF6 and ATF4 pathways at 4 weeks leads to significant protection of the SNc from cell death and restoration of DA levels. Therefore CHOP must also be re-examined as a new therapeutic target for different models of PD. The therapeutic impact of GRP78/BiP protein on CHOP overexpression at 8 weeks is lower then at 4 weeks. This indicates a major cell death in injected SNc at this time point. In general, the BiP therapeutic effect is a "proof of principle" for the idea that reprogramming of apoptotic circuitry in the remaining neurons might turn the balance toward cell survival. It also points to the CHOP protein as a new therapeutic target for PD.

In conclusion, we have demonstrated that α-syn induces a robust UPR *in vivo* in the α-syn rat model of PD. We have verified the importance of the UPR in PD pathogenesis by demonstrating that we could reprogram the ER stress response by overexpression of GRP78/BiP protein. Expression of GRP78/BiP prevents

the death of DA neuron at least in part by reducing the levels of ATF4, ATF6, and CHOP.

MATERIAL AND METHODS

rAAV vectors. All vectors have been packaged in AAV5 capsid and purified as described previously.[24,32–34,38] Virus titers (vector genomes/ml) were determined by dot blot assay[48,49] and were for human wt α-syn: 9.7×10^{12}; GRP78/BiP: 9.1×10^{12}; BiP-Flag: 4×10^{12} GFP: 4.5×10^{13}.

Intracerebral injection of rAAV vectors. All surgical procedures were performed using aseptic techniques and isoflurane gas anesthesia as previously described.[32–34,38] The rats were placed in the stereotaxic frame and injected into the SNc (anterior posterior –5.6 mm, lateral –2.4 mm from bregma and dorsoventral –7.2 mm from dura), through a glass micropipette at a rate of 0.5 μl/minute. Animals were injected with a total of 1.5 μl for single gene or 3 μl for gene combination as previously described[32–34,38] (see also **Supplementary Data** and **Supplementary Figure S5**).

Transfection of SH5-Y5 neuronal cells and immunoblot analysis of cell protein extracts. Transfection was performed using Lipofectamine 2000 according to the manufacturer's protocol. For *in vitro* experiments we used α-syn and pcDNA 3.1BiP[24] plasmids to express human wt α-syn and human BiP/GRP78.

Nucleosome release quantification of apoptosis. We quantified DNA fragmentation resulting from apoptosis. DNA fragmentation occurs as a result of Ca2+- and Mg2+-dependent nuclease cleavage of double-stranded DNA that generates release of mono- and oligonucleosomes, which are complexes tightly associated with the core histones H2A, H2B, H3, and H4. Therefore, we identified nucleosome release levels by a sandwich-enzyme immunoassay using mouse monoclonal antibodies directed against DNA and histones using a Cell Death Detection ELISA kit (Roche Diagnostics, Indianapolis, IN) based on the manufacturer's protocol. At 48 hours post-transfection, the cells were treated with lysis buffer, incubated for 30 minutes, centrifuged at 200*g* for 10 minutes, and 20 μl of the resulting cytoplasmic fraction was used to perform nucleosome release quantitation based on the manufacturer's protocol. Data were normalized to mock-transfected cells.

Immunoprecipitation of protein extract. Immunoprecipitation was done by using a Catch and Release II System (Millipore, Billerica, MA), 500 μg of protein extract, and antibodies against Flag (F7425, rabbit; Sigma, St Louis, MO), α-syn (32-8100, mouse; Invitrogen, Camarillo, CA), GFP (ab1218, mouse; Abcam, Cambridge, MA). The fractions resulting from the immunoprecipitation were denatured and separated on a 12% SDS polyacrylamide gel priori to immunoblotting. Western blots were prepared by standard methods.

Isolation and processing of tissues. Animals were deeply anesthetized by pentobarbital injection. Brains were removed and divided into two parts by a coronal blade cut at approximately –3.5 mm behind bregma. The caudal part containing the SNc was fixed in the ice-cold 4% paraformaldehyde in 0.1 mol/l phosphate buffer, pH 7.4. The fixed part of brains were stored overnight at 4 °C and then transferred into 30% sucrose in 0.1 mol/l phosphate buffer for cryoprotection. Forty-μm thick coronal sections were cut on a freezing stage sliding microtome and processed for immunohistochemistry. The rostral piece of brain tissue was used immediately to dissect the right and left striatum. Tissue samples were weighed, frozen separately on dry ice and kept at –80 °C until assayed. Some brains were used to obtain SNc tissue samples for western blot analysis. Using a Leica surgical microscope at magnification ×40 (ocular ×10, objective lens ×4), the melanin containing substantia nigral region (**Supplementary Figure S6**) was dissected from two consecutive 1 mm coronal slices. Total tissue weight of nigral tissue did not exceed 0.2–0.4 mg.

Immunohistochemistry. For the bright-field microscopy analysis sections were preincubated first with 1% H_2O_2–10% methanol for 15 minutes and then with 5% normal goat serum for 1 hour. Sections were incubated overnight at room temperature with anti-TH (1:2,000; MAB318, mouse; Millipore) or anti-α-syn (1:1,000; 61-787, mouse; BD Laboratories, Sparks, MD) antibodies. Incubation with biotinylated secondary anti-mouse antibody was followed by incubation with avidin–biotin–peroxidase complex (ABC; Vector Laboratories, Burlingame, CA). Reactions were visualized using 3,3-diaminobenzidine as a chromagen.

For confocal microscopy, sections were incubated with primary antibodies against human α-syn (1:1,000; 32-8100, mouse; Invitrogen), Flag (1:500; F7425, rabbit; Sigma), TH (1:1,000; MAB318, mouse; Millipore) and vesicle monoamine transporter-2 (1:400; sc-7721, goat; Santa Cruz Biotechnology, Santa Cruz, CA) and secondary antibodies labeled with DyLight 488, Cy3 and Cy5 (1:100 for all; Jackson Immunoresearch Laboratories, West Grove, PA). The vesicle monoamine transporter-2 or TH antibody was chosen as the DA marker in order to avoid a cross –reaction with other antibodies in any given sample. The sections were examined using a Leica TCS SP5 confocal laser scanning microscope. DyLight 488 fluorescence was visualized by 488-nm excitation with a Kr/Ar laser, and emissions were examined with a band-pass filter for 500–530 nm. For imaging of Cy3 fluorescence, excitation at 543 nm (He/Ne laser) was used, whereas emission was observed at 560–580 nm. Cy5 fluorescence was visualized 633 nm (He/Ne laser) and observed at 660–700 nm. Sequential scanning was used to suppress optical cross talk between the fluorophores in stationary-structure colocalization assays. All manipulations of contrast and illumination on color images as well as color replacement were made using Adobe PhotoShop CS software.

Unbiased stereology. The unbiased stereological estimation of the total number of the TH+ neurons in SNc was performed using the optical fractionator method as described previously.[6,32] This sampling technique is not affected by tissue volume changes and does not require reference volume determinations. Sampling of cells to be counted was performed using the MicroBrightfield StereoInvestigator System. The software was used to delineate the transduction area at 5× on 40-μm sections and generate counting areas of 100×100 μm. A counting frame was placed randomly on the first counting area and systematically moved through all counting areas until the entire delineated area was sampled. Actual counting was performed using a 100× oil objective (NA 1.4). The estimate of the total number of neurons and coefficient of error due to the estimation was calculated according to the optical fractionator formula as previously described.[6,32]

Immunoblotting. Tissues were suspended in 300 μl of lysis buffer (50 mmol/l Tris, pH 7.5, 0.15 mol/l NaCl) containing protease inhibitor cocktail (0.1 mmol/l phenylmethanesulfonylfluoride, 0.5 μg/ml leupeptin, 0.7 μg/ml pepstatin A) (Roche, Indianapolis, IN) and homogenized for 10 seconds. Hundred microliter aliquots were added immediately to 250 μl of 0.1 mol/l $HClO_4$ and stored at –80 °C for subsequent DA measurements. The remainder of each aliquot was adjusted to a final concentration of 1% NP-40, 0.1% SDS, incubated on ice for 30 minutes and centrifuged for 15 minutes at 4 °C. Lysates from each group were pooled and protein concentrations were determined by Bradford. 50 μg of each protein pool was adjusted to 2% SDS, 0.1% 2-mercaptoethanol, heated for 5 minutes at 95 °C, separated on Biorad precast 4–20% SDS-PAGE gradient gel and transferred to PVDF-LFP (Amersham, Piscataway, NJ) membranes for western blotting. Mouse anti-α-syn (1:2,000; BD Transduction Laboratories, Sparks, MD; Zymed Laboratories, San Francisco, CA), mouse anti-GAPDH, and rabbit anti-TH (both 1:2,000; Millipore) were used as recommended by the supplier. Cy5 and Cy3-conjugated goat anti-mouse and rabbit anti-goat secondary antibodies were purchased from GE Bioscience (Piscataway, NJ). Immunoblotted α-syn was detected and quantified with a Typhoon scanner (Amersham) by using purified α-syn-TAP protein as a standard. Westerns used for TH quantitation included GAPDH for normalization. Detection and quantification of main URP markers was done by using infrared secondary antibody, Odyssey an infrared imager (Li-Cor, Lincoln,

NE) and Odyssey quantitative software. Fifty microgram of total protein was used to detect proteins. We used antibodies (all diluted 1:1,000) that detect the stress-induced phosphorylated proteins: anti-peIF2α (sc-101670, rabbit; Santa Cruz Biotechnology), anti-CHOP (sc-735, mouse; Santa Cruz Biotechnology), anti-ATF4 (ab50546-100, mouse; Abcam), anti-ATF6 (ab22280-100, rabbit; Abcam), anti-ATF6 alpha (sc-22799, rabbit; Santa Cruz Biotechnology), ATF6β (N-17) (sc-30596, goat; Santa Cruz Biotechnology) and anti-GRP78/BiP (sc-32138 or sc-1050, both goat; Santa Cruz Biotechnology), anti-XBP1 (sc-32138, goat; Santa Cruz Biotechnology).

The comparative affinity test of anti-α-syn antibody to recognize human and rat α-syn proteins: To obtain recombinant human and rat α-syn protein, HEK293 cells were transfected with plasmid expressing either human α-syn or rat α-syn both tagged with HA and driven under control of the CBA promoter. Forty eight hours after transfection cells were harvested, collected, and lysed in RIPA buffer supplemented with protease inhibitors (Roche). Samples were rotated at 4°C for at least 1 hour, vortexed several times, and centrifuged at 14,000 r.p.m. for 30 minutes. Supernatants were collected in fresh tubes and mixed with 200 µl of anti-HA antibody beads (Roche) and the mixtures were incubated at 4°C over night. Immunoprecipitated samples were then washed three times using 1 ml/sample ice-cold RIPA buffer by mixing beads with RIPA buffer followed centrifugation and removal of the washing buffer using vacuum. Then α-syn-HA proteins were eluted in 200 µl of 0.1 mol/l glycine (pH 2.7). Protein concentrations were determined by Bradford. 2.5, 5, 10, and 20 ng of each protein was adjusted to 2% SDS, 0.1% 2-mercaptoethanol, run on Biorad precast 4–20% SDS-PAGE gradient gel and transferred to PVDF-LFP (Amersham) membrane for western blotting with mouse anti-α-syn antibody (1:2,000; BD Transduction Laboratories, Zymed Laboratories) as describe above. Ponseu S staining was used to confirm equal loading (**Supplementary Figure S1**).

Stiatal DA measurements. DA samples were thawed and the equivalent of 3 mg starting tissue was diluted into 1 ml of 0.1 N HClO$_4$ containing dihydrobenzylamine as an internal control, and thoroughly homogenized. The sample was centrifuged and the supernatant was filtered through a 0.2-µ filter. DA and DOPAC levels were analyzed on a Beckman Gold System using a C18 Waters Symmetry column with an ESA and a Coulochem electrochemical detector equipped with a 5011A analytical cell. The mobile phase was composed as follows: 8.2 mmol/l citric acid, 8.5 mmol/l sodium phosphate monobasic, 0.25 mmol/l EDTA, 0.30 mmol/l sodium octyl sulfate, and 7.0% acetonitrile, pH adjusted to 3.5 then filtered through a 0.2-µm filter membrane. The flow rate was set at 1.5 ml/minutes with a 30-µl injection volume.

Rotational behavior. Drug-induced rotational behavior was measured following an injection of D-amphetamine sulfate (2.5 mg/kg i.p.; Sigma) at 4, 8, and 16 weeks after the viral injection. Rotations were measured during a 90-minute period, and full 360° turns were counted.

Statistical analysis. Data were analyzed using one tailed unpaired *t*-test, one-way ANOVA with Tukey post-test, or two-way ANOVA with Bonferroni post-test using Prism 4 (GraphPad Software, La Jolla, CA). Data are presented as mean ± SE. Unless otherwise specified, all in-text *P* values are from two-way ANOVA.

SUPPLEMENTARY MATERIAL
Figure S1. The comparative affinity test of anti-α-syn antibody to bind recombinant human and rat α-syn-HA fusion proteins of known concentration.
Figure S2. Overexpression of human α-syn in the rat SNc leads to activation of the UPR and elevation of main ER stress markers such as ATF4 and peIF2α (the PERK pathway) and pATF6 (the ATF6 pathway) resulting in overproduction of proapoptotic CHOP protein compared to SNcs injected with GFP.

Figure S3. Measurement of human α syn, and TH expression in the striatum at 4 weeks postinjection.
Figure S4. The graph shows western blot analysis of GRP78/BiP protein expression in nigral tissue of rats injected with rAAV BiP alone (146.9 ± 17.2%, *n* = 3; *P* < 0.05) or rAAV BiP in combination with rAAV α-syn (150.1 ± 13.4%, *n* = 4; *P* < 0.05).
Figure S5. Measurement of human α syn, and TH expression in the striatum at 4 weeks postinjection. Four animals from each group are shown.
Figure S6. Coronal brain slice of a fresh tissue at nigral level.
Supplementary Data.

REFERENCES
1. Fearnley, JM and Lees, AJ (1991). Ageing and Parkinson's disease: substantia nigra regional selectivity. *Brain* **114** (Pt 5): 2283–2301.
2. McGeer, PL, Itagaki, S, Akiyama, H and McGeer, EG (1988). Rate of cell death in parkinsonism indicates active neuropathological process. *Ann Neurol* **24**: 574–576.
3. Auluck, PK, Caraveo, G and Lindquist, S (2010). a-Synuclein: membrane interactions and toxicity in Parkinson's disease. *Annu Rev Cell Dev Biol* **26**: 211–233.
4. Chu, Y and Kordower, JH (2007). Age-associated increases of alpha-synuclein in monkeys and humans are associated with nigrostriatal dopamine depletion: Is this the target for Parkinson's disease? *Neurobiol Dis* **25**: 134–149.
5. Kahle, PJ, Neumann, M, Ozmen, L, Muller, V, Jacobsen, H, Schindzielorz, A *et al.* (2000). Subcellular localization of wild-type and Parkinson's disease-associated mutant alpha -synuclein in human and transgenic mouse brain. *J Neurosci* **20**: 6365–6373.
6. Kirik, D, Rosenblad, C, Burger, C, Lundberg, C, Johansen, TE, Muzyczka, N *et al.* (2002). Parkinson-like neurodegeneration induced by targeted overexpression of alpha-synuclein in the nigrostriatal system. *J Neurosci* **22**: 2780–2791.
7. Masliah, E, Rockenstein, E, Veinbergs, I, Mallory, M, Hashimoto, M, Takeda, A *et al.* (2000). Dopaminergic loss and inclusion body formation in alpha-synuclein mice: implications for neurodegenerative disorders. *Science* **287**: 1265–1269.
8. Lee, AS and Ni, M (2007). ER chaperones in mammalian development and human diseases. *FEBS Lett* **581**: 3641–3651.
9. Lin, JH, Walter, P and Yen, TS (2008). Endoplasmic reticulum stress in disease pathogenesis. *Annu Rev Pathol* **3**: 399–425.
10. Ron, D and Walter, P (2007). Signal integration in the endoplasmic reticulum unfolded protein response. *Nat Rev Mol Cell Biol* **8**: 519–529.
11. Lindholm, D, Wootz, H and Korhonen, L (2006). ER stress and neurodegenerative diseases. *Cell Death Differ* **13**: 385–392.
12. Rao, RV and Bredesen, DE (2004). Misfolded proteins, endoplasmic reticulum stress and neurodegeneration. *Curr Opin Cell Biol* **16**: 653–662.
13. Ron, D and Walter, P (2007). Signal integration in the endoplasmic reticulum unfolded protein response. *Nat Rev Mol Cell Biol* **8**: 519–529.
14. Szegezdi, E, Logue, SE, Gorman, AM and Samali, A (2006). Mediators of endoplasmic reticulum stress-induced apoptosis. *EMBO Rep* **7**: 880–885.
15. Lin, JH, Li, H, Yasumura, D, Cohen, HR, Zhang, C, Panning, B *et al.* (2007). IRE1 signaling affects cell fate during the unfolded protein response. *Science* **318**: 944–949.
16. Rutkowski, DT, Arnold, SM, Miller, CN, Wu, J, Li, J, Gunnison, KM *et al.* (2006). Adaptation to ER stress is mediated by differential stabilities of pro-survival and pro-apoptotic mRNAs and proteins. *PLoS Biol* **4**: e374.
17. Hoozemans, JJ, van Haastert, ES, Eikelenboom, P, de Vos, RA, Rozemuller, JM and Scheper, W (2007). Activation of the unfolded protein response in Parkinson's disease. *Biochem Biophys Res Commun* **354**: 707–711.
18. Smith, WW, Jiang, H, Pei, Z, Tanaka, Y, Morita, H, Sawa, A *et al.* (2005). Endoplasmic reticulum stress and mitochondrial cell death pathways mediate A53T mutant alpha-synuclein-induced toxicity. *Hum Mol Genet* **14**: 3801–3811.
19. Cooper, AA, Gitler, AD, Cashikar, A, Haynes, CM, Hill, KJ, Bhullar, B *et al.* (2006). Alpha-synuclein blocks ER-Golgi traffic and Rab1 rescues neuron loss in Parkinson's models. *Science* **313**: 324–328.
20. Sugeno, N, Takeda, A, Hasegawa, T, Kobayashi, M, Kikuchi, A, Mori, F *et al.* (2008). Serine 129 phosphorylation of alpha-synuclein induces unfolded protein response-mediated cell death. *J Biol Chem* **283**: 23179–23188.
21. Bellucci, A, Navarria, L, Zaltieri, M, Falarti, E, Bodei, S, Sigala, S *et al.* (2011). Induction of the unfolded protein response by a-synuclein in experimental models of Parkinson's disease. *J Neurochem* **116**: 588–605.
22. Gómez-Santos, C, Barrachina, M, Giménez-Xavier, P, Dalfó, E, Ferrer, I and Ambrosio, S (2005). Induction of C/EBP beta and GADD153 expression by dopamine in human neuroblastoma cells. Relationship with alpha-synuclein increase and cell damage. *Brain Res Bull* **65**: 87–95.
23. Matus, S, Lisbona, F, Torres, M, León, C, Thielen, P and Hetz, C (2008). The stress rheostat: an interplay between the unfolded protein response (UPR) and autophagy in neurodegeneration. *Curr Mol Med* **8**: 157–172.

24. Gorbatyuk, MS, Knox, T, LaVail, MM, Gorbatyuk, OS, Noorwez, SM, Hauswirth, WW *et al.* (2010). Restoration of visual function in P23H rhodopsin transgenic rats by gene delivery of BiP/Grp78. *Proc Natl Acad Sci USA* **107**: 5961–5966.

25. Erickson, RR, Dunning, LM and Holtzman, JL (2006). The effect of aging on the chaperone concentrations in the hepatic, endoplasmic reticulum of male rats: the possible role of protein misfolding due to the loss of chaperones in the decline in physiological function seen with age. *J Gerontol A Biol Sci Med Sci* **61**: 435–443.

26. Naidoo, N (2009). The endoplasmic reticulum stress response and aging. *Rev Neurosci* **20**: 23–37.

27. Naidoo, N, Ferber, M, Master, M, Zhu, Y and Pack, AI (2008). Aging impairs the unfolded protein response to sleep deprivation and leads to proapoptotic signaling. *J Neurosci* **28**: 6539–6548.

28. Nuss, JE, Choksi, KB, DeFord, JH and Papaconstantinou, J (2008). Decreased enzyme activities of chaperones PDI and BiP in aged mouse livers. *Biochem Biophys Res Commun* **365**: 355–361.

29. Paz Gavilán, M, Vela, J, Castaño, A, Ramos, B, del Río, JC, Vitorica, J *et al.* (2006). Cellular environment facilitates protein accumulation in aged rat hippocampus. *Neurobiol Aging* **27**: 973–982.

30. Rabek, JP, Boylston, WH 3rd and Papaconstantinou, J (2003). Carbonylation of ER chaperone proteins in aged mouse liver. *Biochem Biophys Res Commun* **305**: 566–572.

31. Chiba-Falek, O, Lopez, GJ and Nussbaum, RL (2006). Levels of alpha-synuclein mRNA in sporadic Parkinson disease patients. *Mov Disord* **21**: 1703–1708.

32. Burger, C, Gorbatyuk, OS, Velardo, MJ, Peden, CS, Williams, P, Zolotukhin, S *et al.* (2004). Recombinant AAV viral vectors pseudotyped with viral capsids from serotypes 1, 2, and 5 display differential efficiency and cell tropism after delivery to different regions of the central nervous system. *Mol Ther* **10**: 302–317.

33. Gorbatyuk, OS, Li, S, Nha Nguyen, F, Manfredsson, FP, Kondrikova, G, Sullivan, LF *et al.* (2010). a-Synuclein expression in rat substantia nigra suppresses phospholipase D2 toxicity and nigral neurodegeneration. *Mol Ther* **18**: 1758–1768.

34. Gorbatyuk, OS, Li, S, Sullivan, LF, Chen, W, Kondrikova, G, Manfredsson, FP *et al.* (2008). The phosphorylation state of Ser-129 in human alpha-synuclein determines neurodegeneration in a rat model of Parkinson disease. *Proc Natl Acad Sci USA* **105**: 763–768.

35. Schapira, AH (2006). Etiology of Parkinson's disease. *Neurology* **66**(10 Suppl 4): S10–S23.

36. Maytin, EV, Ubeda, M, Lin, JC and Habener, JF (2001). Stress-inducible transcription factor CHOP/gadd153 induces apoptosis in mammalian cells via p38 kinase-dependent and -independent mechanisms. *Exp Cell Res* **267**: 193–204.

37. Saha, AR, Ninkina, NN, Hanger, DP, Anderton, BH, Davies, AM and Buchman, VL (2000). Induction of neuronal death by alpha-synuclein. *Eur J Neurosci* **12**: 3073–3077.

38. Gorbatyuk, OS, Li, S, Nash, K, Gorbatyuk, M, Lewin, AS, Sullivan, LF *et al.* (2010). *In vivo* RNAi-mediated alpha-synuclein silencing induces nigrostriatal degeneration. *Mol Ther* **18**: 1450–1457.

39. Ruipérez, V, Darios, F and Davletov, B (2010). Alpha-synuclein, lipids and Parkinson's disease. *Prog Lipid Res* **49**: 420–428.

40. Esteves, AR, Arduíno, DM, Swerdlow, RH, Oliveira, CR and Cardoso, SM (2009). Oxidative stress involvement in alpha-synuclein oligomerization in Parkinson's disease cybrids. *Antioxid Redox Signal* **11**: 439–448.

41. Malhi, H and Kaufman, RJ (2011). Endoplasmic reticulum stress in liver disease. *J Hepatol* **54**: 795–809.

42. Reddy, RK, Mao, C, Baumeister, P, Austin, RC, Kaufman, RJ and Lee, AS (2003). Endoplasmic reticulum chaperone protein GRP78 protects cells from apoptosis induced by topoisomerase inhibitors: role of ATP binding site in suppression of caspase-7 activation. *J Biol Chem* **278**: 20915–20924.

43. Miyake, H, Hara, I, Arakawa, S and Kamidono, S (2000). Stress protein GRP78 prevents apoptosis induced by calcium ionophore, ionomycin, but not by glycosylation inhibitor, tunicamycin, in human prostate cancer cells. *J Cell Biochem* **77**: 396–408.

44. Wang, M, Ye, R, Barron, E, Baumeister, P, Mao, C, Luo, S *et al.* (2010). Essential role of the unfolded protein response regulator GRP78/BiP in protection from neuronal apoptosis. *Cell Death Differ* **17**: 488–498.

45. Leborgne-Castel, N, Jelitto-Van Dooren, EP, Crofts, AJ and Denecke, J (1999). Overexpression of BiP in tobacco alleviates endoplasmic reticulum stress. *Plant Cell* **11**: 459–470.

46. Oida, Y, Izuta, H, Oyagi, A, Shimazawa, M, Kudo, T, Imaizumi, K *et al.* (2008). Induction of BiP, an ER-resident protein, prevents the neuronal death induced by transient forebrain ischemia in gerbil. *Brain Res* **1208**: 217–224.

47. Ryu, EJ, Harding, HP, Angelastro, JM, Vitolo, OV, Ron, D and Greene, LA (2002). Endoplasmic reticulum stress and the unfolded protein response in cellular models of Parkinson's disease. *J Neurosci* **22**: 10690–10698.

48. Zolotukhin, S, Byrne, BJ, Mason, E, Zolotukhin, I, Potter, M, Chesnut, K *et al.* (1999). Recombinant adeno-associated virus purification using novel methods improves infectious titer and yield. *Gene Ther* **6**: 973–985.

49. Zolotukhin, S, Potter, M, Zolotukhin, I, Sakai, Y, Loiler, S, Fraites, TJ Jr *et al.* (2002). Production and purification of serotype 1, 2, and 5 recombinant adeno-associated viral vectors. *Methods* **28**: 158–167.